Available online at www.sciencedirect.com

ScienceDirect

Procedia CIRP 42 (2016) 131 – 136

www.elsevier.com/locate/procedia

18th CIRP Conference on Electro Physical and Chemical Machining (ISEM XVIII)

# Results of Surface Integrity and Fatigue Study of PECM and PEO processed γ-TiAl for Turbine Applications

F. Klocke[a], T. Herrig[a,]*, M. Zeis[a], M. Holsten[a] and A. Klink[a]

[a]*Laboratory for Machine Tools and Production Engineering WZL of RWTH Aachen University, Steinbachstraße 19, 52074 Aachen, Germany*

* Corresponding author. Tel.: +49-241-80-28008; Fax: +49-241-80-22293. *E-mail address:* t.herrig@wzl.rwth-aachen.de

**Abstract**

Gamma Titanium aluminides (γ-TiAl) will play an important role in designing future aero engine components such as turbine blades and blisks. Due to the high heat resistance and low densities these materials are highly suitable for replacing nickel-based alloys in the high pressure compressor and low pressure turbine. Electrochemical machining (ECM) is an attractive process for manufacturing these materials because of the capability of this process to machine materials independent of their mechanical properties. Major advantages of ECM are its process specific characteristics of high material removal rates in combination with almost no tool wear. A possibility to enlarge the field of operation is a heat and corrosion protection layer made out of ceramics for the electrochemical machined turbine blades. One way to produce such a layer is the plasma electrolytic oxidation (PEO).

Aero engine components are subjected to static and dynamic stresses. Component life and failure is greatly affected by aspects of the surface integrity of stressed parts, such as surface roughness values. Precise electrochemical machining (PECM) is capable of producing excellent surface integrity qualities on γ-TiAl without thermally and mechanically affecting the rim zone. In this paper the impact of different processing strategies by ECM as well as by a combination of ECM and PEO on fatigue strength with regard to component life is investigated.



Peer-review under responsibility of the organizing committee of 18th CIRP Conference on Electro Physical and Chemical Machining (ISEM XVIII)

*Keywords:* PECM, γ-TiAl, Surface Integrity, High Cycle Fatigue, FEM

## 1. Introduction

Turbomachinery components, such as turbine blades and blisks, are highly stressed parts. Due to high temperatures and high mechanical loads, the materials used must be highly heat-resistant. Nowadays, these materials are mostly nickel-based alloys like Inconel 718. Nevertheless, the turbomachinery industry pursues new materials, which can meet both higher combustion temperatures and lower component weight requirements, to increase the efficiency of modern aero engines. The outstanding material properties of Gamma titanium aluminides (γ-TiAl) such as high strength-to-weight ratio as well as oxidation and corrosion resistance at high temperatures, make them a promising class of material. Currently there are aero engines that include γ-TiAl blades in the low pressure turbine. The application of γ-TiAl in future aero engines is expected to increase significantly [1-4].

However, γ-TiAl entail some disadvantages regarding their conventional cutting behavior. Due to their low thermal conductivity and brittle nature, an economical manufacturing process via cutting is hardly possible [5, 6]. Therefore, electrochemical machining (ECM) represents an attractive manufacturing alternative. ECM could be a capable manufacturing technology for γ-TiAl as machining is independent of the mechanical properties of the processed material, in combination with high removal rates and no thermally or mechanically affected zone. Due to the non-equidistant working gap the classical direct current DC-ECM process entails some challenges regarding tool design [2]. Further development of the precise electrochemical machining (PECM) enables higher shaping accuracy and excellent



Peer-review under responsibility of the organizing committee of 18th CIRP Conference on Electro Physical and Chemical Machining (ISEM XVIII)
doi:10.1016/j.procir.2016.02.207

surface integrities. Due to the higher secondary processing time of PECM, a combination of ECM roughing and PECM finishing could be an economical manufacturing sequence [3].

Aero engine components must withstand high static and dynamic stresses, see Figure 1. Aerodynamic excitations, mechanical vibrations, airfoil flutter and acoustic fatigue are several sources for potential high cycle fatigue (HCF) damage in turbine engines. Furthermore, HCF is the major source of component failure, especially blades that are subject to these stresses. Hence, lots of investigations for aero engine materials in general, in terms of the influence of manufacturing technologies in particular, on the HCF of component life have been performed [7-13].

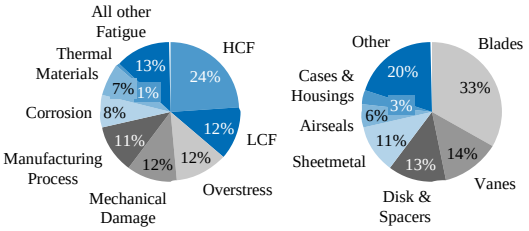


Fig. 1. Left: jet engine component distress mode statistics. Right: distribution of HCF problems by component [7].

For aero engine materials the resistance to fatigue damage is crucial. New material classes like γ-TiAl must be analyzed concerning this matter. Studies on the general fatigue life of γ-TiAl were already performed in the past [5, 14-16]. But only few have focused on HCF tests [12, 13, 17]. Voice et al. [12] have shown a higher HCF and defect tolerance for γ-TiAl alloy Ti-45Al-8Nb-0.2C % (TNB) compared to Ti-45Al-2Mn-2Nb XD and the existing nickel-based blade alloy Inconel 718. Jones et al. [13] analyzed γ-TiAl alloy Ti-47Al-2Nb-2Cr regarding the effects of conventional machining and electropolishing on HCF at 23 °C and 760 °C. At room temperature, the mean fatigue strength was not affected by the surface conditions. At 760 °C turning improved the average fatigue strength by 5 % compared to the electropolished specimens. This resulted from formation of a continuous, crack initiation resistant, recrystallized layer in the outer 30-50 µm of the samples. Sharman et al. [17] studied the influence of cracks, resulting from different manufacturing technologies using the γ-TiAl alloy Ti-45Al-2Mn-2Nb XD on HCF. Electrodischarge textured specimens with crack lengths from 10 µm up to 40 µm showed a substantially reduced fatigue life compared to ECM machined (ECMed) and turned specimens. Turned specimens exhibited the best fatigue life, possibly due to higher compressive residual stresses present in the machined surface. Finally Bannard [18] and Kozak [19] investigated the effect of ECM on fatigue life of titanium and nickel-based alloys. Both detected an influence of intergranular attack from ECM on the fatigue life of the investigated materials.

The literature survey outlines the fact that no analyses on high cycle fatigue of PECM machined (PECMed) materials were performed in the past. Even if the physical process principles of ECM and PECM are similar, no analyzes of the effect of different machining strategies resulting in different surfaces integrities on the HCF behavior were executed. Due to the fact that blades are mainly affected by HCF (Fig. 1) and first aircraft engines, e. g. the GEnx engine, already contains stages with γ-TiAl blades [1], the knowledge of HCF behavior of PECMed γ-TiAl will become very important. Therefore, the aim of this paper is to analyze the effect of different processing strategies by PECM on fatigue strength with regard to component life. Furthermore, PECMed and afterwards plasma electrolytic oxidized (PEO), also known as microarc oxidation (MAO), specimens will be investigated concerning their HCF behavior. PEO is capable of enlarging the field of operation of the γ-TiAl turbine blades by a heat and corrosion protection layer. As the test material, the γ-TiAl Ti-48Al-2Cr-2Nb (GE 48-2-2), which is one actual blade material of the GEnx aircraft engine, is chosen.

**Nomenclature**

| | |
|---|---|
| ECM | Electrochemical Machining |
| EDM | Electrodischarge Machining |
| HCF | High Cycle Fatigue |
| HCFB | High Cycle Fatigue Bending |
| HIP | Hot Isostatically Pressed |
| MAO | Microarc Oxidation |
| $M_b$ | Failure moment |
| $N_1$ | Limit Cycle Number |
| PECM | Precise Electrochemical Machining |
| PEO | Plasma Electrolytic Oxidation |
| R | Radius |
| Ra | Arithmetic Average Surface Roughness |
| U | Voltage |
| f | Oscillation Frequency (PECM) |
| $f_b$ | bending frequency |
| $p_i$ | Electrolyte Pressure Inlet |
| $p_o$ | Electrolyte Pressure Outlet |
| s | Oscillation Stroke |
| t | Specimens thickness |
| $t_{off}$ | Interpulse Period |
| $t_{on}$ | Pulsetime |
| $v_f$ | Feed Rate |
| x | Profile |
| $\alpha_{off}$ | Angle-Off |
| $\alpha_{on}$ | Angle-On |
| γ-TiAl | Gamma Titanium Aluminide |
| κ | Electrolyte Conductivity |
| ν | Poisson's Ratio |
| ρ | Density |
| $\sigma_M$ | Von Mises stress |

## 2. Test material and sample geometry

The investigated γ-TiAl GE 48-2-2 was the first commercial application of γ-TiAl blades in an aircraft engine [1]. Table 1 shows the chemical composition of the material in weight- and atomic-percent. The material was cast in a vertical centrifugal process and afterwards hot isostatically pressed (HIPed).

Table 1. Chemical composition of the examined γ-TiAl GE 48-2-2 [20]

| Ge 48-2-2 | Ti | Al | Cr | Nb |
|---|---|---|---|---|
| at.-% | 48 | 48 | 2 | 2 |
| wt.-% | 58.3 | 34.5 | 2.7 | 4.5 |

For theoretical analyzes of the high cycle fatigue bending (HCFB), some mechanical properties of the material are summarized in Table 2. The literature gives different and varying mechanical data for γ-TiAl in general and for special materials, like GE 48-2-2 only few data are available. Therefore, Table 2 presents the most mentioned data for GE 48-2-2 from the literature survey.

Table 2. Mechanical properties of GE 48-2-2 [12, 14, 20-25]

| | Density ρ / (g/cm³) | Poisson's ratio ν | Young's modulus E / (GPa) |
|---|---|---|---|
| Ge 48-2-2 | 3.9 | 0.27 | 160 |

For HCFB tests the geometry shown in Figure 2 was used. The raw geometry (Fig. 2a) has an overall dimension of 55 mm x 10 mm x 3.5 mm. The specimens were produced by wire electrodischarge machining (wire EDM). The side faces were manufactured with a 3 cut-strategy and afterwards the 12.5 mm radius was polished. The EDM surface (Fig. 2a) was produced with a main cut and afterwards both sides were PECMed resulting in a thickness of 3 mm ±10 µm. The rounded edge (Fig. 2b) is developed due to the compression of electric field lines at sharp edges, which leads to increased material dissolution in general. This behavior will be discussed in detail later on.

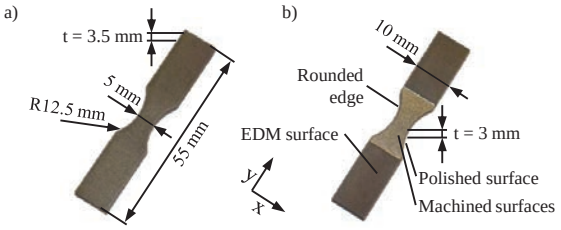


Fig. 2. HCFB specimen geometry, raw material (a) and precise electrochemical machined specimen (b).

## 3. Specimen production and experimental setup

The shown raw specimens were machined on an EMAG Pt smart 400 ECM machine tool. For processing the HCFB specimens a special machining device was constructed, Fig. 3. The device consists of two parts, wherein upper part contains the rectangular cathode and is connected to the mask. Lower part consists of the pressure mask, insulation, specimen positioning, electrolyte in- and outlet and the clamping. The mask forms together with the insulation and specimen the electrolyte flow channel. The mask is fixed on the lower part by clamping. Due to a flexible connector the cathode can oscillate up to 2 mm. The oscillation stroke enables the plunging depth and the cathode oscillation, which is required for the PECM.

The machining device was enabled to remove 250 µm from each side of the relevant areas of the specimens for the

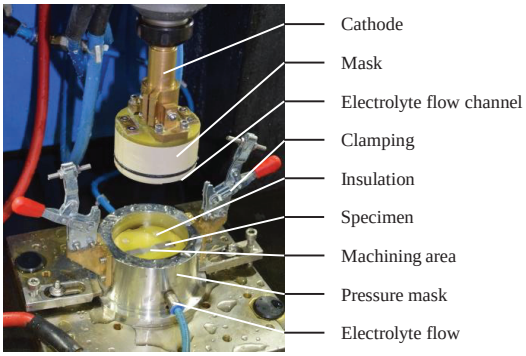


Fig. 3. PECM device for HCFB specimen.

HCFB test (Fig. 2b). Specimens were produced within a tolerance of ±10 µm. The manufacturing of the specimens were performed with two different machining strategies, whereby the difference of the strategies consisted of a different feed rate. Different feed rates result in different current densities and, thus, in different surface roughness values. Lower current densities can occur for example during processing side gaps, like fillets of blades. Strategy 1 was determined to achieve best surface roughness in GE 48-2-2. The surface roughness of specimens manufactured with strategy 1 was Ra ≈ 1.3 µm. Due to different dissolution behavior of the phases better surface roughness are hardly achievable in typical (near-) lamellar or (near-) equiaxed γ-TiAl microstructures [17, 26-28]. Strategy 2 achieved a surface roughness Ra ≈ 2.2 µm. Table 3 summarizes the applied machining parameters.

Table 3. Machining parameters

| Unit | Strategy 1 | Strategy 2 |
|---|---|---|
| Electrolyte | $NaNO_3$ | |
| Electrolyte conductivity κ | 120 mS/cm at 20 °C | |
| Voltage U | 17 V | |
| Electrolyte pressure inlet $p_i$ | 3 bar | |
| Electrolyte pressure outlet $p_o$ | 1.5 bar | |
| Feed rate $v_f$ | 0.113 mm/min | 0.053 mm/min |
| Angle-on $\alpha_{on}$ | 130° | |
| Angle-off $\alpha_{off}$ | 220° | |
| Oscillation frequency f | 50 Hz | |
| Oscillation stroke s | 0.1 mm | |
| Pulsetime $t_{on}$ | 0.6 ms | |
| Interpulse period $t_{off}$ | 1 ms | |
| Rectangular cathode shape | 10.5 x 18 mm² | |
| Machining depth | 0.25 mm | |

To investigate specimens with a ceramic layer for heat and corrosion protection, samples were manufactured with strategy 1 and afterwards PEO machined (PEOed). The PEO-layer was applied by the company Meotec GmbH & Co. KG. The ceramic protection layer is still in the development phase. Therefore, the influence on the mechanical properties of the application material was investigated. The protection layer thickness was roughly about 10 – 20 µm. The process did not

deposit the whole layer, most of it was transformed base material. The PEO process increased the overall thickness of the specimens by less than 6 µm on each side. The surface roughness is strongly affected by the PEO process so that a roughness of Ra ≈ 4.1 µm was obtained. Further information about the PEO or MAO process can be seen in Kurze [29].

Figure 4a shows the set up for the HCFB tests. Investigations were conducted on a Rumul Cracktronic 160. The bending machine tool works at full resonance of the sample geometry. After installation of the specimen, a defined sinusoidal moment with an amplitude of $M_b$ and a mean value of zero is applied to the oscillating clamping. All investigations were performed at room temperature.

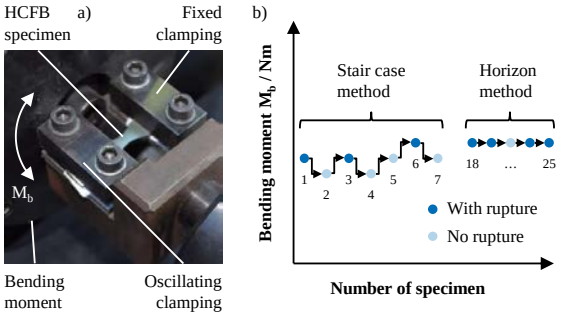


Fig. 4. HCFB test set up (a). Example of stair case and horizon method (b).

For analyzing the HCF of the manufactured material the stair case method with an additional horizon method was chosen. Figure 4b illustrates this approach. A limit cycle number of $N_1 = 5 \cdot 10^6$ cycles was set. If the specimen exceeded $N_1$, the bending moment was increased by $\Delta M_b = 0.125$ Nm for the next specimen. If the sample ruptured, the bending moment was decreased by $\Delta M_b$. Such a combination of the stair case method and the horizon method enables a closer look to the transition zone and combines the specific advantages of both test methods. This method is qualified for high cycle fatigue tests to evaluate the 10 %, 50 % and 90 % failure probability in the transition area [30]. According to the sample geometry the bending frequency occurs to 68 Hz < $f_b$ < 73 Hz. In total 25 specimens were investigated per series. In Welling [8, 9] and Klocke et al. [10] more information about this test setup and procedure can be found.

## 4. Rim zone analysis and test results

In order to analyze the influence of the manufacturing process and thus the surface integrity properties on the HCFB behavior, it is indispensable to have a closer look at the rim zones. Figure 5 shows the microscopy inspections of the machined and PEOed rim zones. As expected no thermal influence of the PECM process (Fig. 5a, b) can be seen at all [2, 27, 28]. PECMed and PEOed specimen (Fig. 5c) showed the γ-TiAl base material with the ceramic protection layer.

Cross sections shown in Figure 5a and 5b were etched to illustrate the microstructure, whereas the cross section of Figure 5c was let untreated to clarify the PEO-layer.

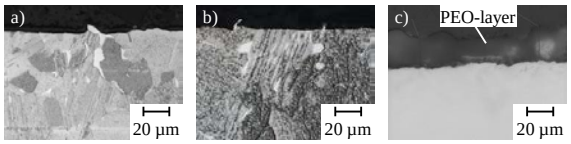


Fig. 5. Cross-sections of PECMed strategy 1(a), PECMed strategy 2 (b) and PECMed and PEOed specimen (c).

The different surface roughness values of PECM strategy 1 and 2 are hardly noticeable in the cross sections. Even the SEM pictures of the machined surfaces (Figure 6) hardly exhibit any differences between the two PECM strategies. Nevertheless, the inhomogeneous dissolution behavior of the GE-48-2-2 is clearly recognizable. The areas sticking out could have a notch effect on the HCFB behavior.

The PEO-layer increased the surface roughness of the specimens, which is clearly visible in Fig. 5c and Fig. 6. Furthermore, the SEM analyzes of the PEO surface showed the typical properties of a PEO-layer with some pores. However, the ceramic-film is a continuous layer. As well as in the PECM surfaces the rough areas possibly affect the HCF.

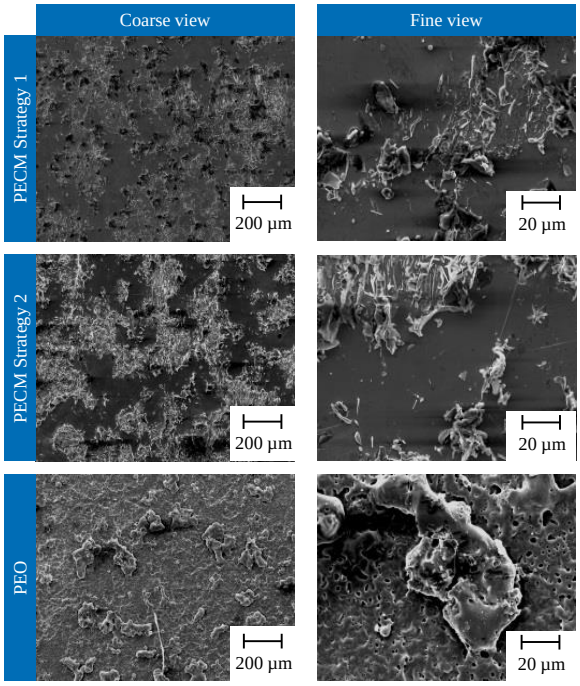


Fig. 6. SEM pictures of machined surfaces.

In Figure 7a, the results of the HCFB tests are shown. These results have been statistically calculated by the SAFD-software [30]. The failure moment for all three series showed a high correlation for all failure probabilities. For safety critical parts, such as turbine blades, the fatigue limit with a failure probability of 10 % is more meaningful than the 50 % or 90 % failure probability. The PECMed samples with strategy 2 exhibit the highest failure moment $M_b = 2.14$ Nm compared to PECMed strategy 1 $M_b = 2.02$ Nm and PEOed

$M_b$ = 1.97 Nm. Only with respect to the surfaces roughness this result was not expected and is discussed later on. Nevertheless, Welling [8, 9] examined wire EDMed and broached Inconel 718 specimens and had a failure moment $M_b$ = 2.2 Nm for 50 % failure probability. The γ-TiAl GE 48-2-2 machined with Strategy 1 withstands a failure moment $M_b$ = 2.25 Nm for 50 % failure probability; machined with Strategy 2 correspond to a failure moment of $M_b$ = 2.31 Nm. The PEOed specimens have an average value of $M_b$ = 2.16 Nm. This means PECMed GE 48-2-2 is in principle at the same level of broached or wire EDM machined Inconel 718 concerning the failure moment.

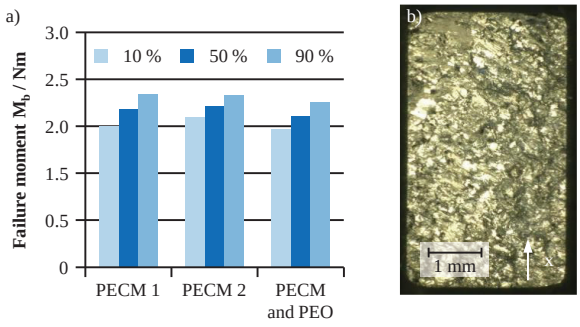


Fig. 7. Failure moment for different failure probabilities (a) and fracture surface of PECMed specimen (b).

Figure 7b shows a micrograph of a typical fracture surface of a PECMed specimen. Corresponding to the brittle behavior of γ-TiAl the ruptured specimens show evidence of brittle fracture. During examining the fracture surfaces of the different machined specimen conspicuous feautures regarding the rounded edges were recognized. The specimens manufactured with the PECM strategy 1 exhibit an average rounded edge of 180 µm radius, whereas the specimens machined with strategy 2 exhibit an average rounded edge of 220 µm radius.

## 5. Theoretical analysis of the sample geometry

In order to analyze the geometrical influence of the specimen's radius on the failure moment, FEM-simulations

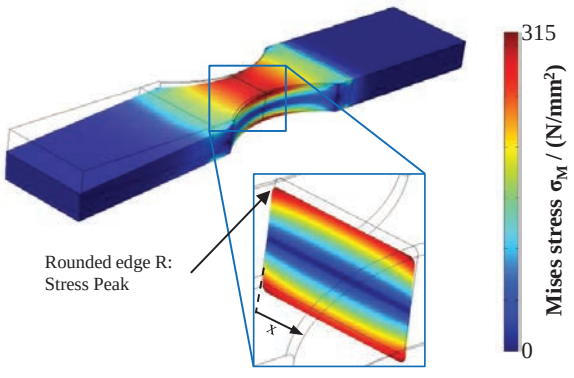


Fig. 8. Distribution of Mieses stress on test geometry.

were conducted. The impact of different radii on the Mises stress at the surface was studied. The material properties shown in Table 2 were set. On the cross section of the neck, mesh size was defined by 28 µm for each rounded edge and a max. of 50 µm mesh size on the flat surfaces. Two non-deformable plates at one end of the specimen define the fixed clamping. A bending moment $M_b$ = 2.2 Nm was applied with a third rigid plate on the opposite side of the specimen.

Figure 8 shows the result of Mises stress at the whole specimen's surface and in the cross section at the neck. Recognizable are the stress peaks at the rounded edges. To study these peaks, Figure 9 shows the Mises stress as a function of the radii along the cross-sectional profile. The stress at the edge increases with decreasing radius, but a larger radius corresponds to a higher stress in the middle of the profile.

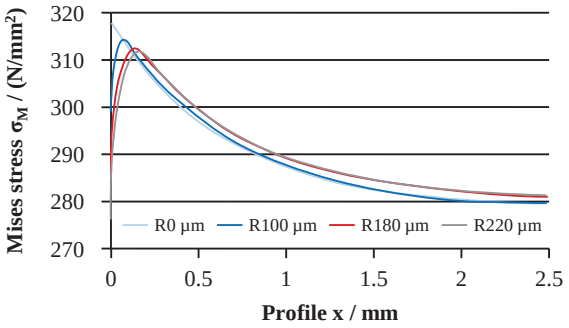


Fig. 9. Calculated von Mieses Stresses of different radii as a function of the symmetrical cross-section surface profile.

These stress peaks could be crack initiators for specimen rupture. Due to the brittle fracture, the initiation point of the rupture cannot be readily located. This means that the influence of the radius size could mask the influence of the specimen's surface integrity on the HCF. However, the specimens withstand the above mentioned failure moment while the fatigue stress limit is in the range of the calculated Mises stress (Fig. 9, $\sigma_M$ = 280 – 318 N/mm²). Other sample geometries could enhance the measured failure moment respectively the measured fatigue stress limit, but the determined failure moment represents a minimum. For the ductile material Inconel 718, Welling [8, 9] has shown that the starting point of the crack was on the top of the surface and was not hence affected by the rounded edge.

This behavior could explain the higher failure moment $M_b$ of the specimens machined by strategy 2. In Figure 9 the different Mises stresses for 180 µm and 220 µm radii are shown. A slightly flattened peak of the 220 µm radius is recognizable, which could be the reason for the higher failure moment.

## 6. Summary and conclusions

In this paper investigations on the HCF behavior of PECM- and PEO machined GE 48-2-2 are presented. The production of specimens and their investigation regarding the

surface integrity are discussed. The specimens showed the typical thermally and mechanically non-affected ECM surface. Furthermore, HCF test procedure was described. The different specimens exhibited a roughly equal failure moment $M_b \approx 2.2$ Nm for 50 % failure probability and, thus, showed an equal HCF as broached or wire EDM Inconel 718. For low pressure turbine and high pressure compressor γ-TiAl is in principle a possible replacement material for Inconel 718 in the turbomachinery industry. Regarding the low density of γ-TiAl the specific HCF is higher than Inconel 718. The HCF behavior of GE 48-2-2 is not affected by representative PEO protection-layer. Nevertheless, studies on the sample geometry exhibited some disadvantages regarding the rounded edge size. Especially for brittle material, which does not allow the localization of the rupture starting point, this sample geometry must be critically reviewed. But due to the stress peak at the radius the determined fatigue moment can be seen as a minimum to withstand failure moment. These results can also be transferred to the automotive industry, such as turbocharger applications.

## Acknowledgements

The work was partially funded by the following projekts: The authors would like to thank the Central Innovation Program SME (Zentrales Innovationsprogramm Mittelstand – ZIM BMWI) for the support (funding number KF2120329SU3) and furthermore the collaboration partner Meotec GmbH & Co. KG. In addition some aspects have been developed within the project ETurbo. This research and development project is funded by the German Federal Ministry of Education and Research (BMBF) within the Framework Concept “Research for Tomorrow’s Production” (funding number 02PN2071) and managed by the Project Management Agency Karlsruhe (PTKA). The author is responsible for the contents of this publication.

## References

[1] Bewlay, B.P., Weimer, M., Kelly, T., Suzuki, A., Subramanian, P.R. The Science, Technology, and Implementation of TiAl Alloys in Commercial Aircraft Engines. MRS Proc. 1516, 2013.

[2] Zeis, M. Modellierung des Abtragprozesses der elektrochemischen Senkbearbeitung von Triebwerksschaufeln. Dissertation RWTH Aachen, 2015.

[3] Klocke, F., Klink, A., Veselovac, D., Aspinwall, D.K., Soo, S.L., Schmidt, M., Schilp, J., Levy, G., Kruth, J.-P. Turbomachinery component manufacture by application of electrochemical, electro-physical and photonic processes. CIRP Annals - Manufacturing Technology 63 (2), 703–726, 2014.

[4] Dimiduk, D. Gamma titanium aluminide alloys - an assessment within the competition of aerospace structural materials. Materials Science and Engineering: A 263 (2), 281–288, 1999.

[5] Aspinwall, D.K., Dewes, R.C., Mantle, A.L. The Machining of Gamma-TiAl Intermetallic Alloys. CIRP Annals - Manufacturing Technology 54 (1), 99–104, 2005.

[6] Klocke, F., Settineri, L., Lung, D., Priarone, P.C., Arft, M. High performance cutting of gamma titanium aluminides: Influence of lubricoolant strategy on tool wear and surface integrity. Wear 2013 (302), 1136–1144, 2013.

[7] Cowles, B.A. High cycle fatigue in aircraft gas turbines-an industry perspective. Int J Fract 80 (2-3), 147–163, 1996.

[8] Welling, D. Results of Surface Integrity and Fatigue Study of Wire-EDM Compared to Broaching and Grinding for Demanding Jet Engine Components Made of Inconel 718. Procedia CIRP 13, 339–344, 2014.

[9] Welling, D. Wire EDM for the manufacture of fir tree slots in nickel-Based alloys for jet engine components. Dissertation RWTH Aachen, 2015, in press.

[10] Klocke, F., Welling, D., Dieckmann, J. Comparison of Grinding and Wire EDM Concerning Fatigue Strength and Surface Integrity of Machined Ti6Al4V Components. Procedia Engineering 19, 2011.

[11] Soo, S.L., Antar, M.T., Aspinwall, D.K., Sage, C., Cuttell, M., Perez, R., Winn, A.J. The Effect of Wire Electrical Discharge Machining on the Fatigue Life of Ti-6Al-2Sn-4Zr-6Mo Aerospace Alloy. Procedia CIRP 6, 215–21, 20139.

[12] Voice, W.E., Henderson, M., Shelton, E.F., Wu, X. Gamma titanium aluminide, TNB. Intermetallics 13 (9), 959–964, 2005.

[13] Jones, P., Eylon, D. Effects of conventional machining on high cycle fatigue behavior of the intermetallic alloy Ti-47Al-2Nb-2Cr (at.%). Materials Science and Engineering: A 263 (2), 296 ‐ 304, 1999.

[14] Gebhard, S., Peters, P., Roth-Fagaraseanu, D., Turley, F., Voggenreiter, H. Particle impact damage in the gamma based TiAl alloy TNB-V3B produced via three different processing routes. Materials Science and Engineering: A 527 (21-22), 5883–5891, 2010.

[15] Mantle, A., Aspinwall, D. Surface integrity and fatigue life of turned gamma titanium aluminide. Journal of Materials Processing Technology 72 (3), 413–420, 1997.

[16] Brookes, S.P., Kühn, H.-J., Skrotzki, B., Klingelhöffer, H., Sievert, R., Pfetzing, J., Peter, D., Eggeler, G. Axial–torsional thermomechanical fatigue of a near-γ TiAl-alloy. Materials Science and Engineering: A 527 (16-17), 3829–3839, 2010.

[17] Sharman, A., Aspinwall, D., Dewes, R., Clifton, D., Bowen, P. The effects of machined workpiece surface integrity on the fatigue life of γ-titanium aluminide. International Journal of Machine Tools and Manufacture 41 (11), 1681–1685, 2001.

[18] Bannard, J. Effect of surface finish obtained by electrochemical machining on the fatigue life of some titanium alloys. J Appl Electrochem 4 (3), 229–234, 1974.

[19] Kozak, J., The Effect of Electrochemical Machining on the Fatigue Strength of Heat Resistance Alloys. Fatigue of Aircraft Structures, 2011.

[20] Bartolotta, P., Barrett, J., Kelly, T., Smashey, R., The use of cast Ti-48Al-2Cr-2Nb in jet engines. JOM 49 (5), 48–50, 1997.

[21] Lou, J., Soboyejo, W.O. An investigation of the effects of loading rate on resistance-curve behavior and toughening in cast lamellar gamma-based titanium aluminides. Metall and Mat Trans A 32 (2), 325–337, 2001.

[22] Kim, Y.-W. Intermetallic alloys based on gamma titanium aluminide. JOM 41 (7), 24–30, 1989.

[23] Kim, Y.-W. Ordered Intermetallic Alloys, Part III: Gamma Titanium Aluminides. JOM, 1994.

[24] Franzén, S.F., Karlsson, J., Dehoff, R., Ackelid, U., Rios, O., Parish, C., Peters, W. Microstructural Properties of Gamma Titanium Aluminide Manufactured by Electron Beam Melting. The Minerals, Metals & Materials Society (TMS) (Volume 3), 455–462, 2011.

[25] Martienssen, W., Warlimont, H. Springer handbook of condensed matter and materials data. Springer, Heidelberg, New York, 2005.

[26] Klocke, F., Herrig, T., Zeis, M., Klink, A. Experimental Research on the Electrochemical Machinability of selected γ-TiAl alloys for the manufacture of future Aero Engine Components. Procedia CIRP 35, 50-54, 2015.

[27] Clifton, D., Mount, A., Jardine, D., Roth, R. Electrochemical machining of gamma titanium aluminide intermetallics. Journal of Materials Processing Technology 108 (3), 338–348, 2001.

[28] Klocke, F., Herrig, T., Zeis, M., Klink, A. Comparison of the Electrochemical Machinability of Electron Beam Melted (EBM) and Casted Gamma Titanium Aluminide TNB-V5. CAPE 23, Edinburgh, 2015.

[29] Kurze, P. Herstellung, Charakterisierung und Anwendung von Al2O3-Schichten insbesondere auf Aluminium- und Eisenwerkstoffen. Technische Hochschule Karl-Marx-Stadt, Habilitation, 1982.

[30] Klubberg, F., Hempen, M., Schäfer, H.J. Software SAFD 5.5 IWM der RWTH Aachen, 2006.